

Supplementary information for Vishwanathan et al.

October 25, 2016

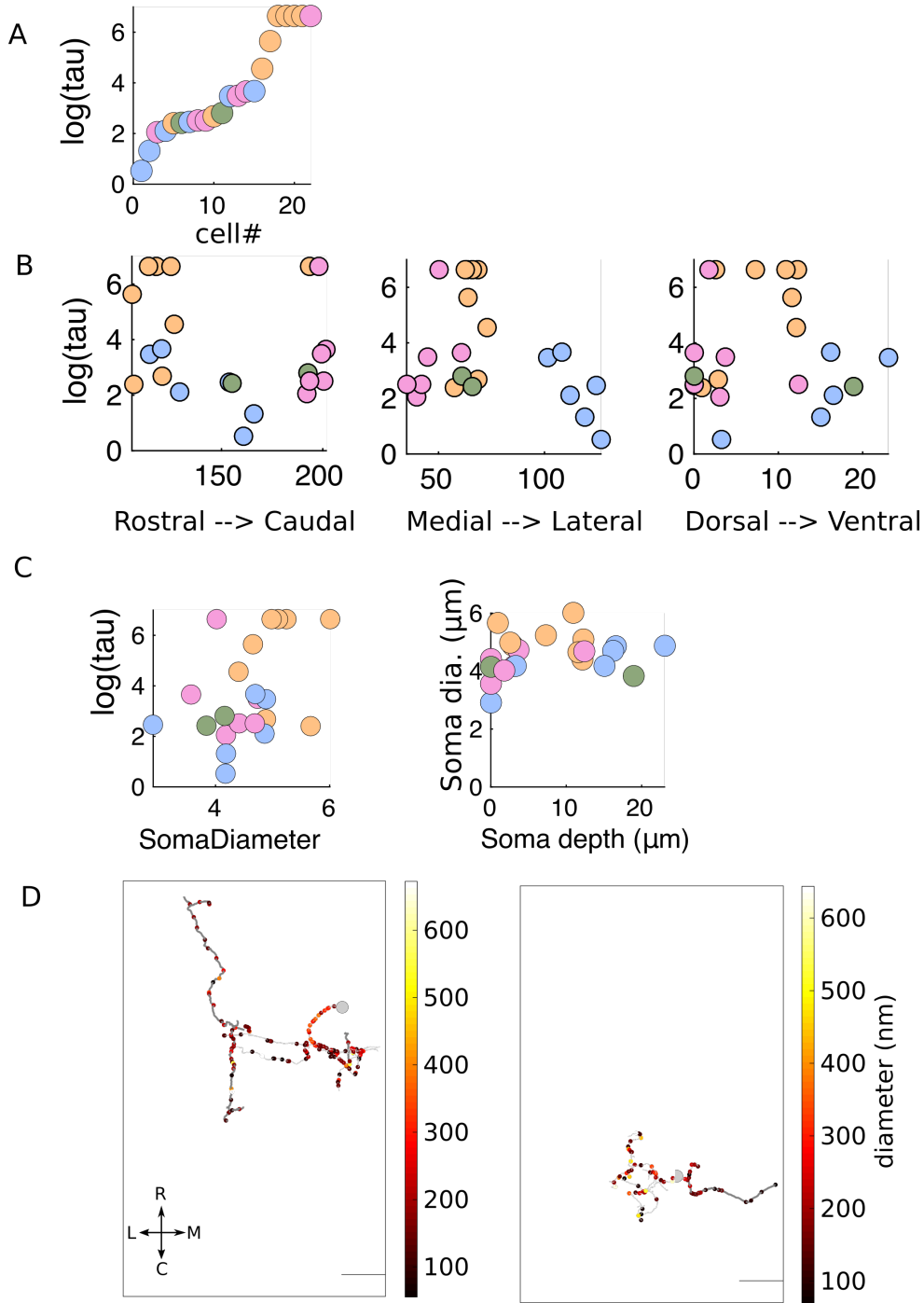


Figure 1: Supplementary figure 1

(A) Graded levels of persistent activity of the 22 reconstructed integrator neurons.

(B) Persistence time constants along the rostro-caudal, medio-lateral and dorso-ventral axis respectively.

(C) (left) Integrator neuron somata diameter versus the depth along the dorso-ventral axis.

(right) Persistent times of integrator neuron versus somal diameter versus

(D) Diameter profiles along ipsi only (left) and contra only (right) integrator cells. Location of each dot represents the thickness of the neurite.

Large grey circle represents the somata of the cell. All thin neurites are dendritic and all thick neurites are axonal. Scale bar $20\mu\text{m}$.

Colors represent the group that the cell belong to. (Pink - ipsi only, Green - Ipsi-contra, Orange - contra only and Blue - unknown).

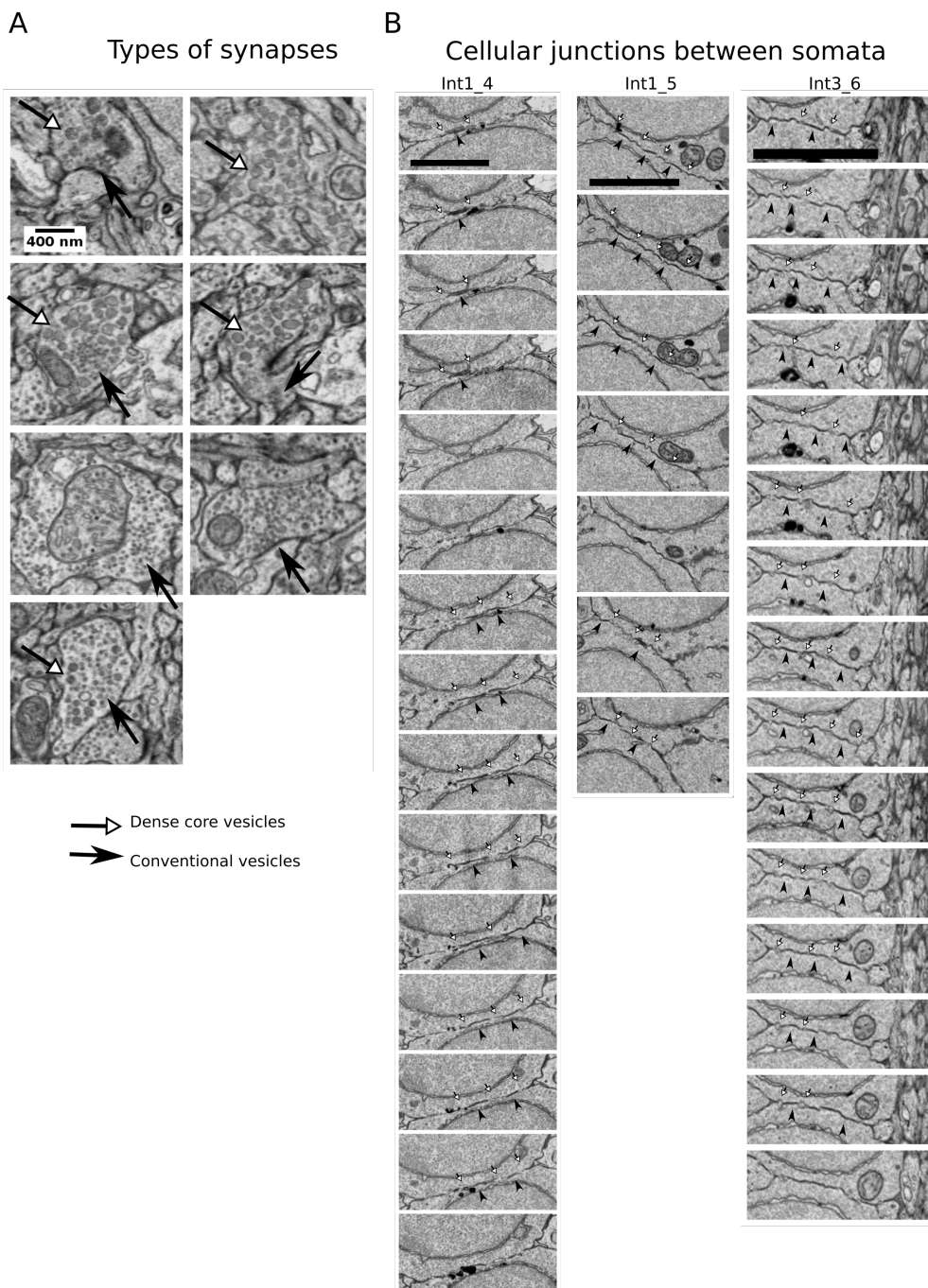


Figure 2: Supplementary figure 2

(A) Examples of types of synapses in the imaged volume. Closed arrows show conventional synapses and open arrows shows dense core vesicles within the same bouton.

(B) Successive images from cellular junctions between cells somata. Closed arrow head shows tight junction indicated by darkening of the membrane in the same location in multiple sections. Open arrows show the separation of the membrane by the lack of darkening. Scale bar 500nm

Location of abducens nuclei

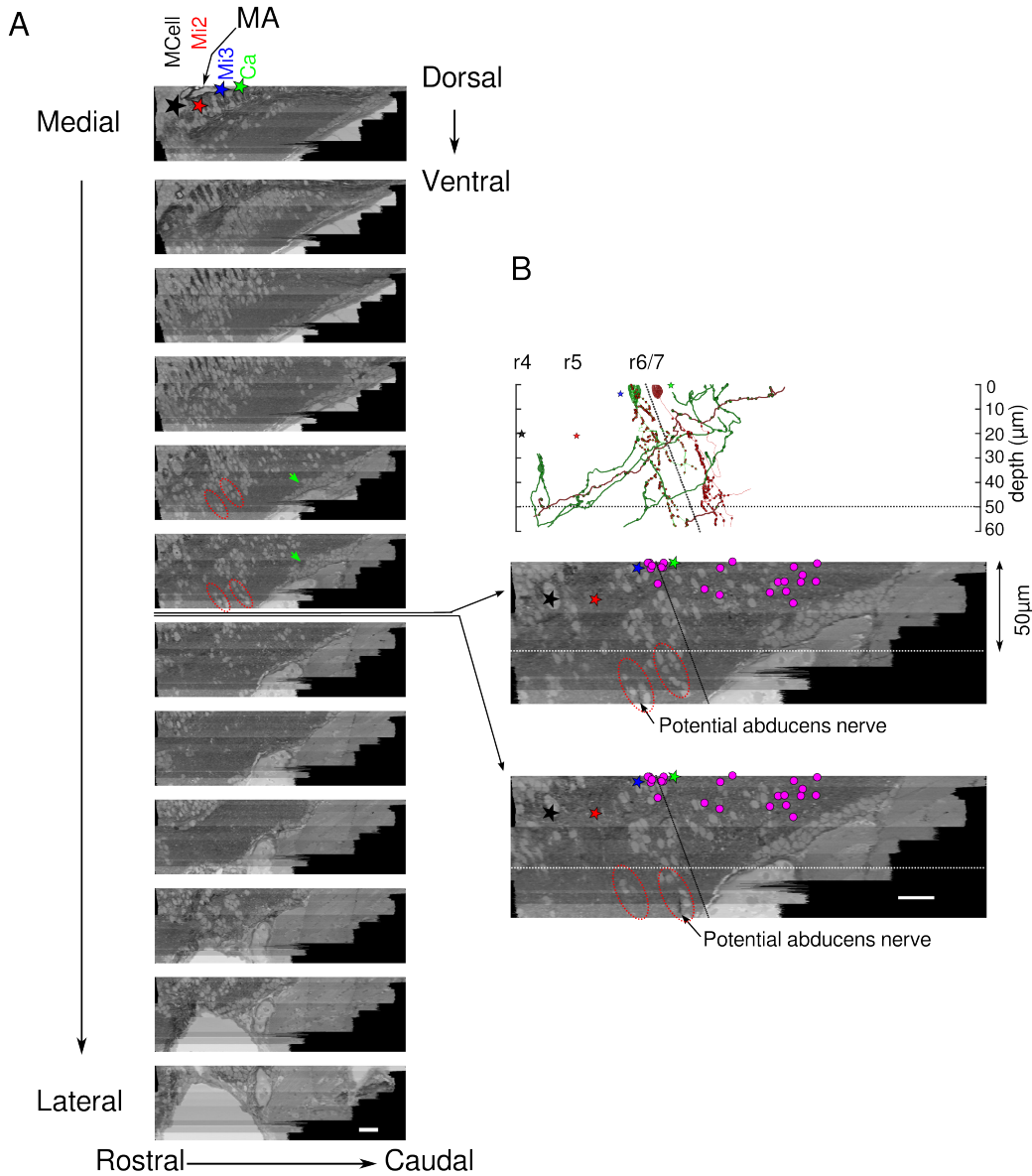


Figure 3: Supplementary figure 3

(A) Location of abducens nuclei from serial of low-res EM images. The frames are ordered from medial to lateral orientation every 10 μ m. Rhombomeres r4-7 were identified based on the location of the reticulo-spinal cells (MCell, Mi2, Mi3 and Ca). Dotted white line is 50 μ m ventral to the Mauthner axon plane. Red dotted circles show the potential locations of both abducens nuclei. Green arrow shows the location of the inferior olive. MA -Mauthner Axon. Scale bar 20 μ m.

(B) Lateral view of two ipsilaterally projecting integrator neurons that sending axonal projections towards the abducens nuclei. The axons project to the same depth as the abducens nuclei (dotted black line). Black dotted line is the border between r6 and r7, with tilt calculated based on [1, 2]. Scale bar 20 μ m.

Cell ID

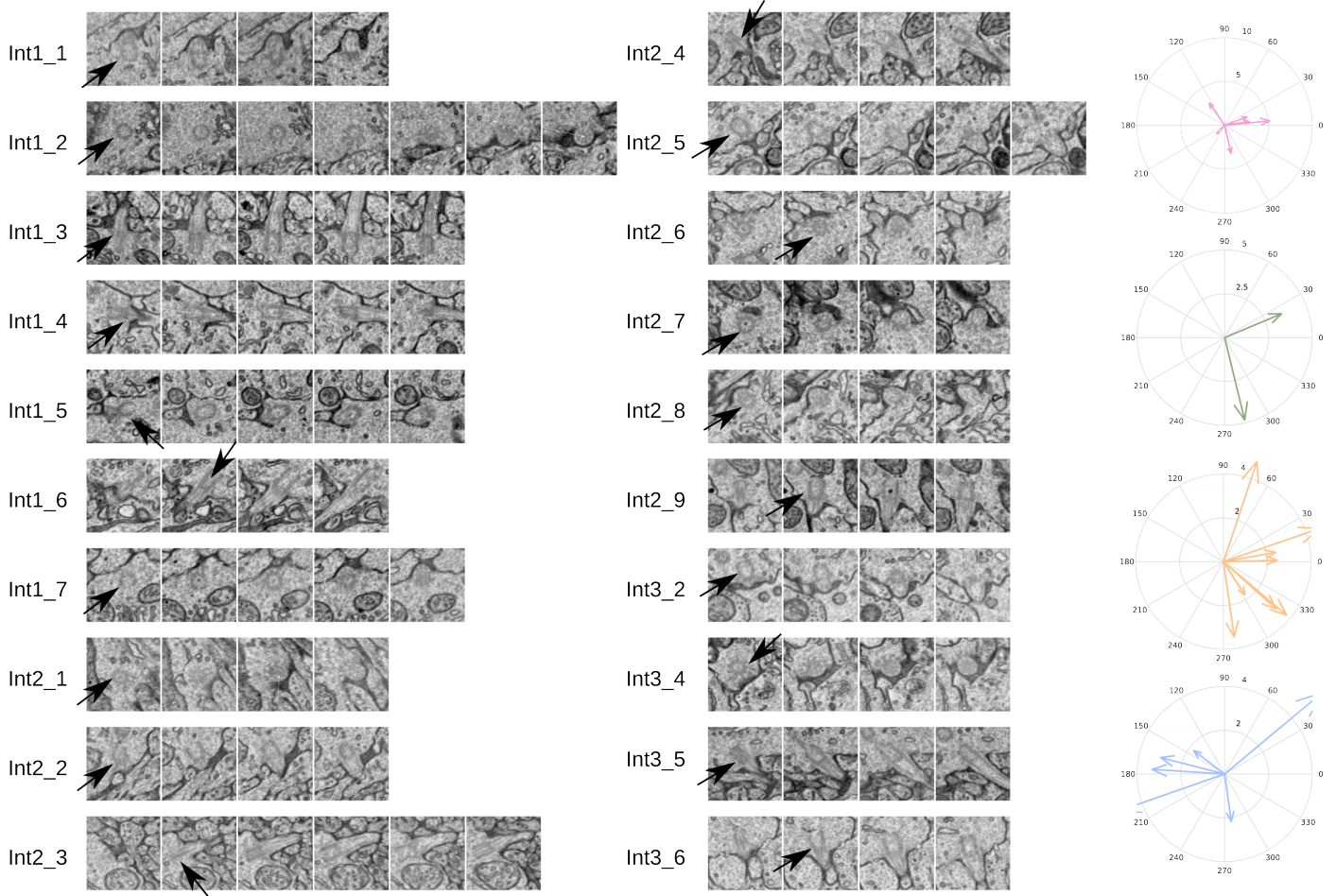


Figure 4: Supplementary figure 4

(A) Primary cilium of every integrator cell identified in the volume. The primary cilium is visible in multiple sections by the presence of a microtubule rich neurite (arrow) that emerges very close to the Golgi complex of the cells.

(B) Orientation of the primary cilium for the four cell groups.

Colors represent the group that the cell belong to. (Pink - ipsi only, Green - Ipsi-contra, Orange - contra only and Blue - unknown).

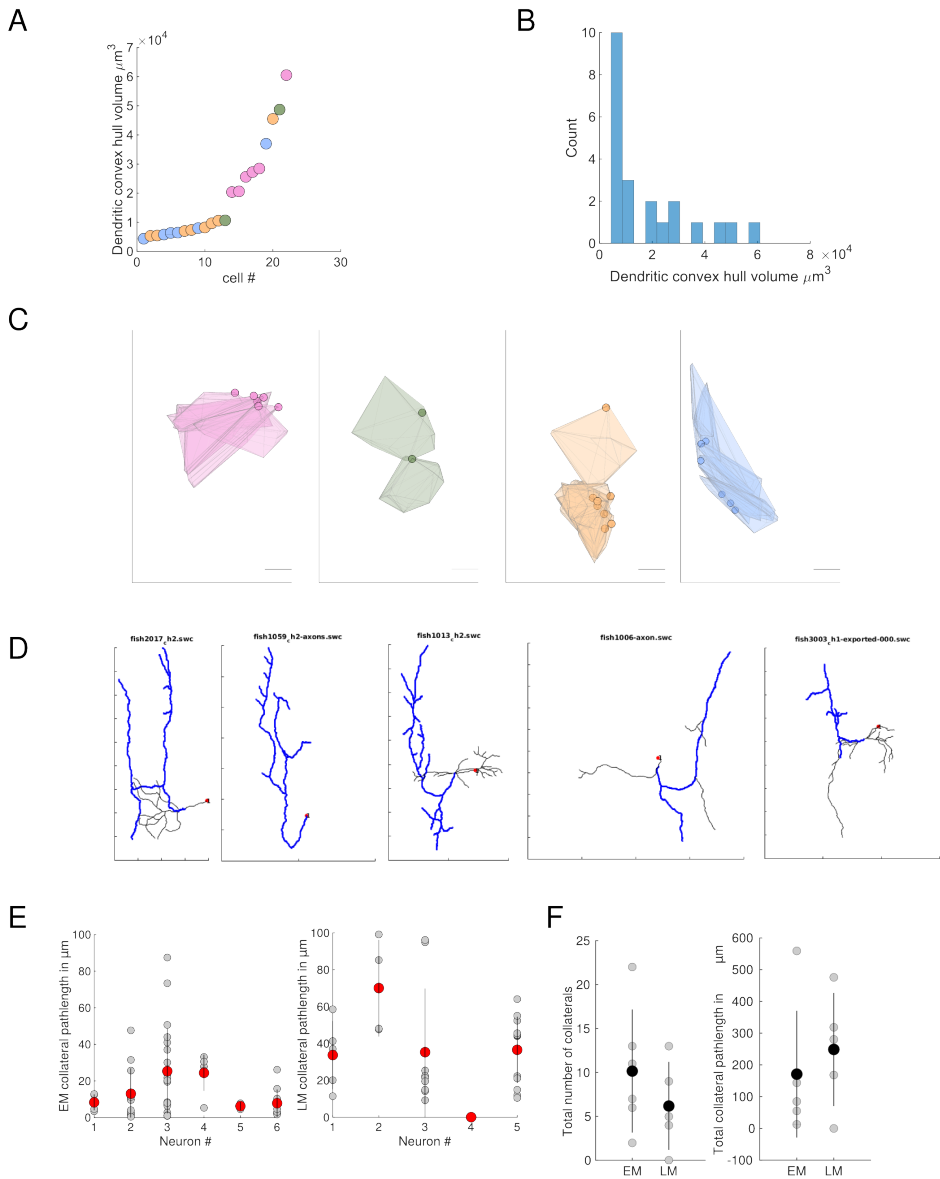


Figure 5: Supplementary figure 5

(A) Convex hull volume of dendrites of all integrator cells, color coded by the cell group that they belong to.

(B) Distribution of the convex hull volume of the integrator cells.

(C) Convex hulls of all cells color coded by the group that they belong to.

(D) Traces of integrator cells from light microscopic dye fills, with ipsilateral projecting axons that were used for comparison with EM cells.

(E) Collateral path length of all EM , LM cells respectively. Grey circles are for individual collaterals for each cells, and red circle is the mean \pm standard deviation.

(F) Number of Collaterals and pathlength of collaterals for EM and LM traces.

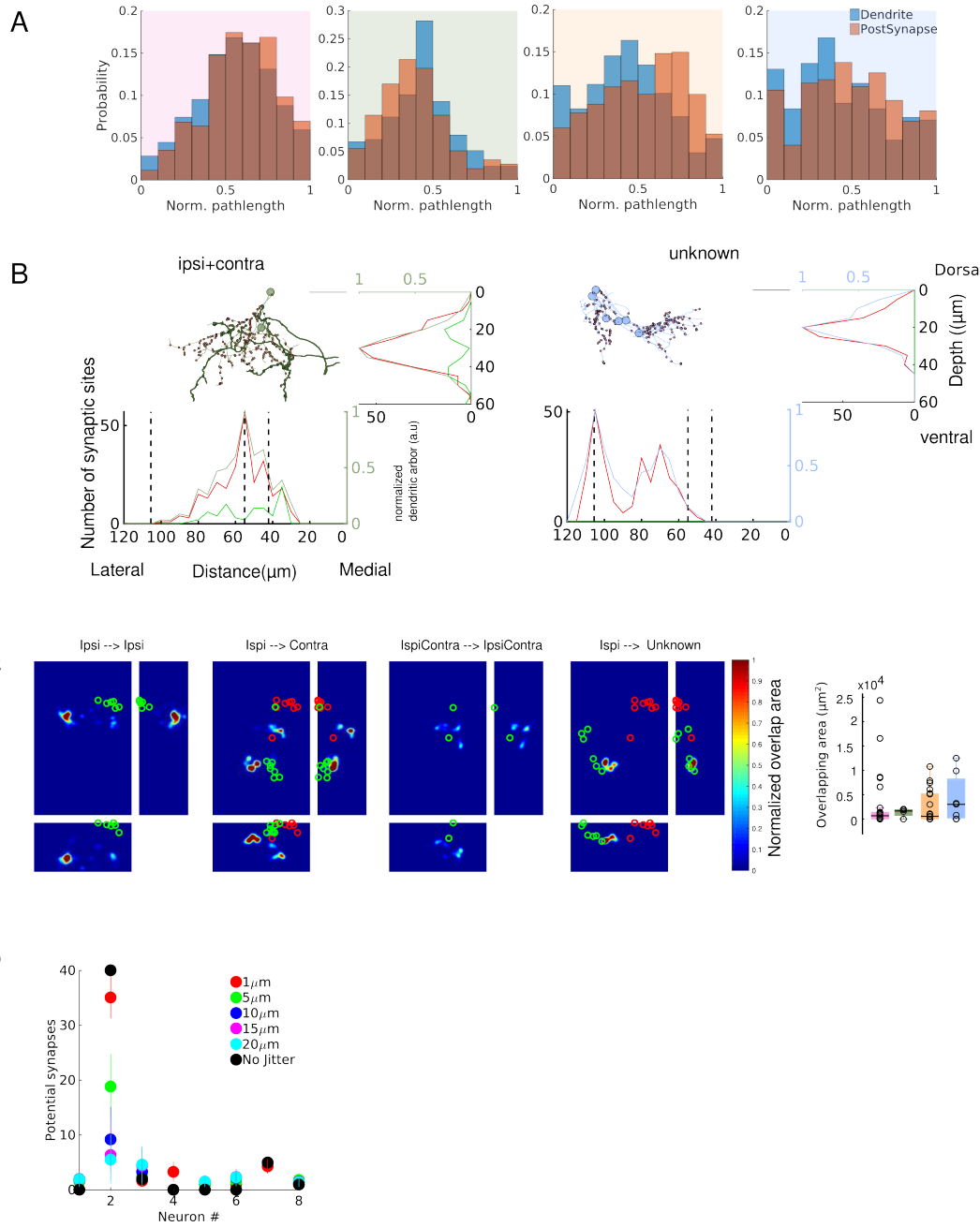


Figure 6: Supplementary figure 6

(A) Distribution of the normalized postsynaptic pathlength and the distribution of the normalized dendritic pathlength for all four groups.

(B) Depth stratification of all cells in each group. For each panel, below the trace of all cells is the stratification of the dendrites (red) and axons (green) along the mediolateral axis. To the right is the stratification along the dorso-ventral axis. Black dotted line are the locations of the stripes from figure 4.

(C) Overlap of axons and dendrites between axons and dendrites. Box plot with overlapping areas for the four groups.

(D) Jittering of the potential synapses for all integrator cells with axons.

Cell group	# Cells	Total length (μm)	Axonal length (μm)	Dendritic length (μm)	Convex hull volume (μm^3)	Axon diameters (μm)	Dendrite diameter (μm)	Axon initiation site (μm)
Ipsi. only	6	661.89 \pm 253.57	269.74 \pm 244.41	392.14 \pm 66.31	3.04 \times 10 ⁴	0.21 \pm 0.15	0.25 \pm 0.15	36.68 \pm 12.74
Ipsi-contra.	2	696.59 \pm 200.92	277.28 \pm 22.08	419.30 \pm 178.84	2.96 \times 10 ⁴	0.2 \pm 0.11	0.21 \pm 0.12	29.21 \pm 8.06
Contra. only	8	358.13 \pm 62.76	65.72 \pm 15.24	292.41 \pm 69.75	1.23 \times 10 ⁴	0.16 \pm 0.08	0.22 \pm 0.12	12.89 \pm 6.07
unknown	6	221.47 \pm 48.7	NA	221.47 \pm 48.70	1.13 \times 10 ⁴	NA	0.22 \pm 0.12	

Table 1: Anatomical features of integrator neurons

Supplementary experimental procedure

Two-photon calcium imaging.

Nacre mutant zebrafish larvae, X days of age, was anesthetized in 100 or 200 mg/L tricaine-methanesulfonate (MS222, VWR TCT0941-025G) for about 1 minute and then quickly mounted dorsal side up with droplets of 1.7% low temperature agarose (Sigma A0701-100G) in the lid of a 35mm petri dish containing a bed of hardened 1% agarose (Invitrogen 15510-027). The larva was then covered in 50 mg/L MS222. The larva was bulk-loaded [3, 4] with calcium sensitive dye Oregon Green 488 BAPTA-1 AM (5 mM, in DMSO with 5% pluronic, Invitrogen, O-6807) by inserting a capillary through the dorsal skin surface over the lateral edge of the right side of the hindbrain just caudal to the cerebellum, at ~30° decline relative to the dorsal surface.

The integrator neurons were identified in a manner similar to a previously described method [5, 1]. Briefly, correlations for every pixel over a 5min acquisition period was determined for eye position and eye velocity. A region-of-Interest (ROI) was then drawn over the pixels where the majority were correlated one of these variables. The fluorescence was reported as change in fluorescence for each frame to the average fluorescence, divided by the average. Saccadic fluorescence traces were displayed over an 8 sec window starting 1 sec before the end of the saccade. The firing rates were computed over a 6 second fixation period beginning 1 sec after the end of the saccade. The firing rates were computed by deconvolving the average fluorescent traces with a calcium impulse response function (CIRF) as described previously [6]. The integrator time constants were calculated by fitting an exponential function (Matlab *ezfit*) to the firing rates. The time constants for the fits were capped at 100 sec.

Serial section electron microscopy.

The animal was immersed in a fixative of 1% paraformaldehyde and 1% glutaraldehyde buffered in 0.1M cacodylate buffer and 4% sucrose for 72 hrs. Then it was thoroughly washed in 0.1M cacodylate buffer before staining. The tissue was stained using a conventional ROTO procedure [7]. Briefly, it was stained in 1% reduced osmium tetroxide with potassium ferrocyanide for 2 hr on ice. It was then washed 4x 30 min with 0.1M cacodylate buffer, also on ice. This was then followed by amplification in 1% sodium thiocarbohydroazide (TCH) for 15min followed by 3x5 min washes in water and another incubation in 1% osmium tetroxide for 1 hr. The tissue was then washed 3x15 min in water and incubated with 1% aqueous uranyl acetate overnight. The following day the tissue was washed 3x15 min in water and dehydrated with a series of ethanol, followed by propylene oxide (PO). The tissue was then infiltrated in decreasing gradients of PO and EPON for 24 hrs and baked for 48 hrs at 60 C. The EPON based resin was tailored to have low viscosity, to help with better infiltration for this tissue. Following hardening, the tissue block face was coarsely trimmed and a rectangular mesa was defined for serial sectioning. Care was taken to orient the specimen to permit sectioning along the horizontal axis. Serial sections from the above animal were collected approximately from the level of the Mauthner cell at a thickness of 45 nm. . The serial sections were then adhered to a silicon wafer, using double sided carbon tape (TEDpella), the wafers were coated with a thin film of carbon to make them conductive.

Registration of light microscope and electron microscope volumes

The EM images were aligned using the trakEM2 plugin in Fiji [8]. Briefly, individual images were imported into the TrakEM2 framework and montaged, first, using affine transforms, followed by elastic transforms. The images were then registered using a similar approach, where the first pass was performed using affine transforms, followed by elastic transforms . All the alignment was performed on a machine with 32 virtual cores and 120GB RAM.

To locate the cells that were involved in the integrator circuit, we made use of the fact that large, gross morphological features were easily identified in both the LM and EM stacks. Once enough such features were identified in the LM stack, we located these same landmarks in the high-res EM stack. Each pair of landmarks (one from the LM volume and one from the EM volume) was then used to calculate a global affine transform that was applied to transform the LM volume to be overlaid on the EM volume using the TrakEM2 plugin in Fiji [8]. Following this registration, we were able to reliable locate the same cells from the LM and the EM volumes.

Reconstructions

Two expert tracers reconstructed the cells beginning from the cell bodies in an independent manner. During the tracing process, one of the expert tracers annotated all pre and postsynaptic sites for each cells. The skeletonized tree structure was exported from TrakEM2 as *.swc files. These trees were then imported into Matlab using custom scripts to import .swc files as trees. The traces of the two tracers were compared by a third reviewer. The third reviewer, independently reviewed points of disagreement and decided which points of disagreement were either over-reconstructed or were under-reconstructed. In some cases, the traces were re-visited by the tracers if it was needed.

Analysis

All traces were exported as .swc files from TrakEM2. All tree lengths was reported as pathlengths unless noted otherwise. Similarly, all lengths to a pre- or post synaptic site was reported as pathlengths. We defined the axon initiation site was annotated as the parent node of the first presynaptic site. One cell from ipsi-only group was defined as an axon, based on diameter of the axons and the 'bare' initial segment. All neurites that were not axonal were defined as dendritic. All nodes of the tree were thus divided as axonal nodes or dendritic nodes. Pathlengths were then generated for a tree over all axonal nodes or all dendritic nodes, and the length of the tree was the sum of all axonal length and dendritic length. A collateral was defined as all those segments of an axon, that emerged from the central axonal tree. All tree

nodes that were axonal were then divided as those that were part of a collateral and those that were not. Following this, pathlengths and numbers were calculated by treating those nodes like any other. The completeness of cells was decided based on the number of neurites that exited the cells.

The diameter of the trees was generated by drawing a line segment across the cross-section of the tree at a random location along the tree. Many such line segments were drawn across the entire extent of the tree, where the tracer was blinded to the fact whether the neurite was an axon or a dendrite. The measurements were then separated as dendritic diameter or axonal diameter after all the trees were measured in this manner. The values were reported as a mean across all dendritic or axonal measures for a tree.

Arbor densities of the dendrites was computed by projecting all the axonal or dendritic nodes along the desired plane and reported in a normalized scale. Arbor volumes were computed using the Matlab function *convhull*. To infer the neurotransmitter identity from the stripe organization of the cell bodies, we annotated the location of all the cell bodies from a low-resolution stack. The cell density was then computed by projecting all the cells along the desired axis. This process picked out the peaks that were visible in the EM images. The location of a stripe was defined as the local peak that emerged from the cell density projecting analysis. The planar organization of the postsynapses and presynapses were fit to a plane using the *planefit* function, available on the Matlab central repository.

To locate the border of r6/7 we followed a similar approach that was performed previous using light microscopic imaging and the expression of the *hox* genes [9, 1, 2]. Reticulospinal cells were identified based on the ultrastructure, that was very different form the remaining cells in the area. These cells were rich in mitochondria and gave rise to a large myelinated axon that joined the remaining fibers along the midline. We fit a plane to the reticulospinal neurons, and identified a point on this plane that bisected Mi3 and Ca. This point was move by $0.37\mu m$ caudally for every micron ventrally.

References

- [1] Kayvon Daie, Mark S Goldman, and Emre R F Aksay. Spatial patterns of persistent neural activity vary with the behavioral context of short-term memory. *Neuron*, 85(4):847–860, February 2015.
- [2] Melanie M Lee, Aristides B Arrenberg, and Emre R F Aksay. A Structural and Genotypic Scaffold Underlying Temporal Integration. *The journal of neuroscience*, 35(20):7903–7920, May 2015.
- [3] E Brustein, N Marandi, Y Kovalchuk, P Drapeau, and A Konnerth. "In vivo" monitoring of neuronal network activity in zebrafish by two-photon Ca²⁺ imaging. *Pflügers Archiv*, 446(6):766–773, 2003.
- [4] D Smetters, A Majewska, and R Yuste. Detecting action potentials in neuronal populations with calcium imaging. *Methods (San Diego, Calif.)*, 18(2):215–221, June 1999.
- [5] Andrew Miri, Kayvon Daie, Aristides B Arrenberg, Herwig Baier, Emre Aksay, and David W Tank. Spatial gradients and multidimensional dynamics in a neural integrator circuit. *Nature neuroscience*, 14(9):1150–1159, September 2011.
- [6] Andrew Miri, Kayvon Daie, Rebecca D Burdine, Emre Aksay, and David W Tank. Regression-Based Identification of Behavior-Encoding Neurons During Large-Scale Optical Imaging of Neural Activity at Cellular Resolution. *Journal of Neurophysiology*, 105(2):964–980, February 2011.
- [7] Juan Carlos Tapia, Narayanan Kasthuri, Kenneth J Hayworth, Richard Schalek, Jeff W Lichtman, Stephen J Smith, and JoAnn Buchanan. High-contrast en bloc staining of neuronal tissue for field emission scanning electron microscopy. *Nature Protocols*, 7(2):193–206, February 2012.
- [8] Albert Cardona, Stephan Saalfeld, Johannes Schindelin, Ignacio Arganda-Carreras, Stephan Preibisch, Mark Longair, Pavel Tomancak, Volker Hartenstein, and Rodney J Douglas. TrakEM2 software for neural circuit reconstruction. *PLoS ONE*, 7(6):e38011, 2012.
- [9] Leung-Hang Ma, Charlotte L Grove, and Robert Baker. Development of oculomotor circuitry independent of hox3 genes. *Nature communications*, 5:4221, 2014.